doi:10.7289/V5JH3J4S

GSICS Global Space-based Inter-Calibration System **Quarterly** **V5 No. 4 2011**

CMA • CNES • EUMETSAT • IMD• ISRO• JAXA•JMA • KMA • NASA • NIST • NOAA • ROSHYDROMET• USGS• WMO

http://gsics.wmo.int *Dr. Fangfang Yu, Editor*

Special Issues on the Vicarious Calibration of GEO Solar Reflective Channel s

This is the first of two special issues of the GSICS Quarterly Newsletter that will focus on the methods used to calibrate Geostationary (GEO) solar reflective sensors. These instruments experience continuous degradation in space and lack onboard calibration systems. Vicarious calibration is the only way to provide accurate radiometric data for the visible and near-infrared channels of these satellites. Even with the inclusion of onboard calibration devices on the next-generation GEO instruments, vicarious calibration will continue to play an important role in verifying and serving as a backup for the onboard systems. A variety of vicarious calibration methods are used by the GSICS community to provide post-launch calibration coefficients for the GEO solar reflective channels. These include satellite observation and radiative transfer modeling of cloud, desert, and ocean targets, inter-calibration with reference sensors, and time-series observations of stable extra-terrestrial targets. The Algorithm Theoretical Basis Documents (ATBD) of each method can be found at the GSICS ATBD wiki webpage: https://gsics.nesdis.noaa.gov/wiki/Development/AtbdCentral.
- The Editor

The NASA-Langley Deep Convective Cloud Technique to Calibrate GEOs

The Deep Convective Cloud (DCC) technique is an earth view invariant target approach designed to provide vicarious geostationary (GEO) visible sensor calibration coefficients for both stability monitoring and the transfer of the polar-orbiting Aqua-MODIS – which has an onboard calibration system – reference calibration. DCC are bright tropical predictable targets, which act as solar diffusers. DCC are found over all the GEO domains providing a common target for all GEO and LEO based sensors. DCC tops are at the tropopause, ensuring very little water vapor absorption across the spectra. Collectively DCC have a nearly Lambertian bidirectional reflectance distribution function (BDRF) and predictable TOA albedos. There is little inter-annual, seasonal, or spatial DCC natural variability.

To transfer of the calibration of one sensor to another using the DCC technique is accomplished by using the same DCC population to calibrate both sensors. GSICS has agreed to use Aqua-MODIS band-1 as the calibration reference, since it is more stable than Terra-MODIS. By limiting the identified DCC to the Aqua-MODIS overpass time and over the GEO domain, as well as using the same identification criteria, the same DCC are captured for both the GEO and Low Earth Orbit (LEO) sensors. The Aqua-MODIS DCC reference radiance can then be transferred to the GEO sensor after applying a Spectral Band Adjustment Factor (SBAF).

DCC are easily identified by a pixel level 11 µm brightness temperature less than 205°K, with a spatial uniformity of surrounding pixels of less than 1°K in the IR and 3% in the visible. Limiting the solar and view angles to less than 40° ensures that the BDRF effects are small. A simple ±20° latitude domain guarantees only tropical convection is considered. The success of this method depends on capturing a very large population of DCC pixels. DCC identification is dependent on good IR calibration, which is sufficient for most GEO sensors, and visible/IR co-registration.

The DCC pixel level radiances are converted to overhead sun and nadir condition using the CERES Angular Dependence Model (ADM) for overcast ice clouds for very large optical depths. The mode of the Probability Distribution Function (PDF), based on all pixel level DCC radiances over the month, provides the monthly DCC nadir radiance. Uniform monthly PDFs over the lifetime of the instrument provide confidence that the technique is applied properly to GOES-13 as shown in Figure 1 (below) upper panel. The lower panel shows the degradation of the GOES-13 visible band in counts.

To transfer the absolute calibration of Aqua-MODIS using DCC, the 9-year mean of Aqua-MODIS DCC monthly nadir radiances is corrected spectrally to match the GEO spectral response function. The GEO gain is then the factor needed to multiply the GEO DCC nadir count minus the space count to equal the SBAF corrected Aqua-MODIS DCC nadir radiance. SBAF is derived from a 2^{nd} order regression of the pseudo MODIS and GEO reflectances based on the SCIAMACHY classified DCC footprint hyper-spectral reflectances. For DCC the SBAF is usually between 0.99 and 1.0 for GEO visible bands with a standard error less than 0.75%.

For GOES-13 the DCC calibration transfer uncertainty is 1.2%, based on small changes in DCC temperature threshold and acquisition time. For best results the Aqua-MODIS equivalent GEO brightness temperature should be used. More information can be obtained from the NASA-Langley GSICS DCC ATBD.

(by Dr. David Doelling, [NASA])

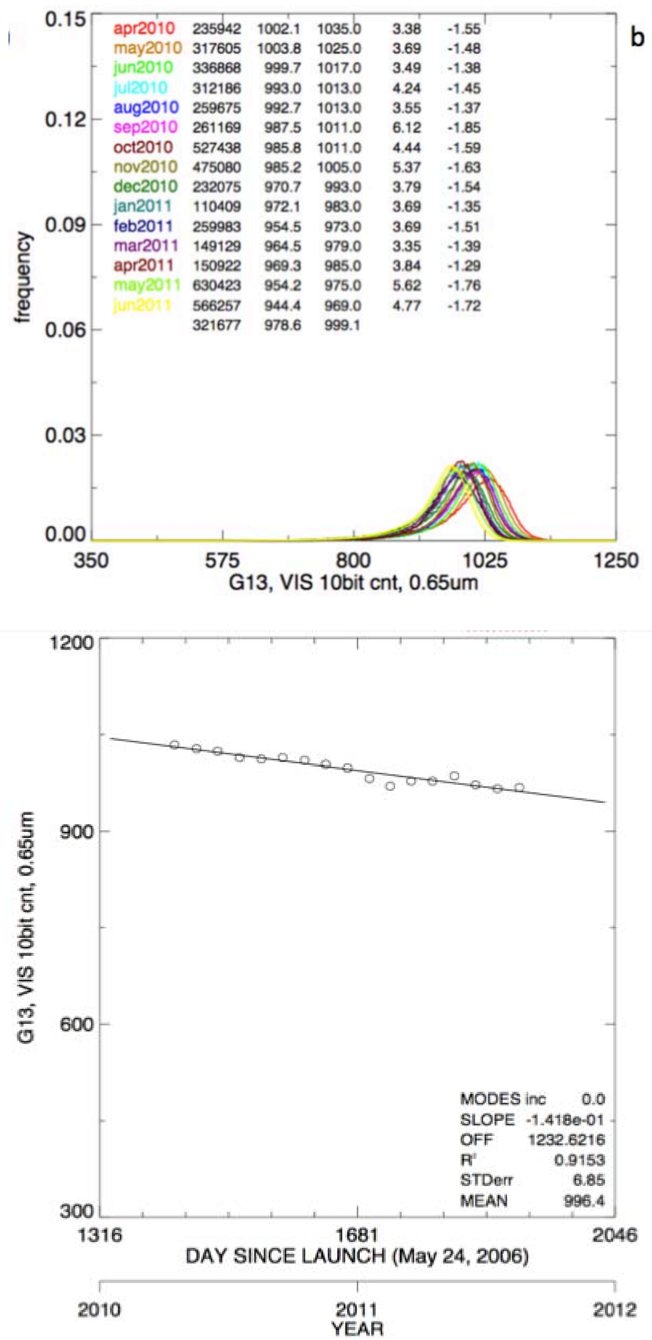

Figure 1: Upper panel: Monthly PDF of DCC nadir pixel radiances of GOES-13 during April 2010 to June 2011. Lower panel: Monthly GOES-13 visible count based on the mode of the PDF.

The NASA-Langley Ray-match Technique to Calibrate GEOs

The ray-matching technique is a vicarious approach of transferring calibration from a well-calibrated satellite sensor to another sensor using coincident, co-angled, and collocated pixels. The GSICS calibration standard is Aqua-MODIS, since it is more stable than Terra-MODIS and better characterized. This technique also provides an assessment of the sensor linearity if the entire dynamic range is sampled. Sun-synchronous orbits ground tracks intersect near the poles, ~ 14 times per day. The ground track intersect pixel is known as the simultaneous nadir overpass (SNO) measurement. For geostationary (GEO), most ray-matches occur near the GEO sub-satellite point, providing opportunities of sampling very bright clouds suitable for ray-matching. This study focuses on GEO/MODIS visible ray-matching but can easily be applied to any two satellite pairs of similar spectral bands.

To spatially match the pixel footprints between two sensors and to reduce the effects of navigation and time mismatch errors, a 30° by 40° latitude by longitude GEO domain, with a 0.5° by 0.5° grid resolution, centered at the GEO sub-satellite point is used to average the pixel level radiances. A 15-minute time match threshold is used. The matching threshold for solar, viewing, and azimuth angles between the two sensors are 5°, 10° and 15°, respectively. Also a sun glint probability of less then 10% is applied. In order to reduce the effects of the Spectral Band Adjustment Factor (SBAF) error only regions over ocean are used. To increase the number of ocean regions the domain can be shifted in longitude, especially to encompass optically thick high clouds, usually found in the ITCZ. All coincident, co-angled, and collocated regional sensor radiances are regressed monthly.

The SBAF is derived from SCIAMACHY footprint hyper-spectral radiances by computing pseudo GEO and MODIS reflectances over the ocean-only GEO domain. A 2nd order regression takes into account the spectral variation from dark radiances, corresponding to clear ocean to very bright radiances associated with deep convective clouds. For MODIS/GEO visible bands, SBAF is on the order of 1-5% with a spectral uncertainty from 0.3-2% for nearly broadband sensors, since MODIS band 1 is very narrow. A consistency check was performed by deriving SBAF over the GOES-12 domain separately for land and ocean. These SBAFs were applied to the ocean and land GOES-12/Terra-MODIS regressions during September 2009. The land/ocean gain difference was reduced from 5.3% to 0.3% after applying the SBAFs and the land-offset was adjusted from 47 to 30 counts, very close to the published space count of 29.

The monthly GEO gain is then the factor needed to convert the GEO count minus the space count to equal the Aqua-MODIS SBAF radiance based on the monthly regression. Figure 1 upper panel shows the November 2007 regression of Aqua-MODIS with Meteosat-9. The lower panel shows the Meteosat-9 monthly gains as a function of time.

Ray-matching can be validated by putting Terra-MODIS on the same radiometric scale as Aqua-MODIS band 1 using Simoultaneous Nadir Overpass (SNO) measurements over the poles. Then Terra and Aqua-MODIS can independently calibrate GEO. For Meteosat-9 the Aqua/Terra gain difference is 0.91% and the degradation is nearly identical at 1.24%/decade. This round-robin of ray-matching validates the robustness of the technique. More information can be obtained from the NASA-Langley GSICS ray-matching ATBD.

(by Dr. David Doelling, [NASA])

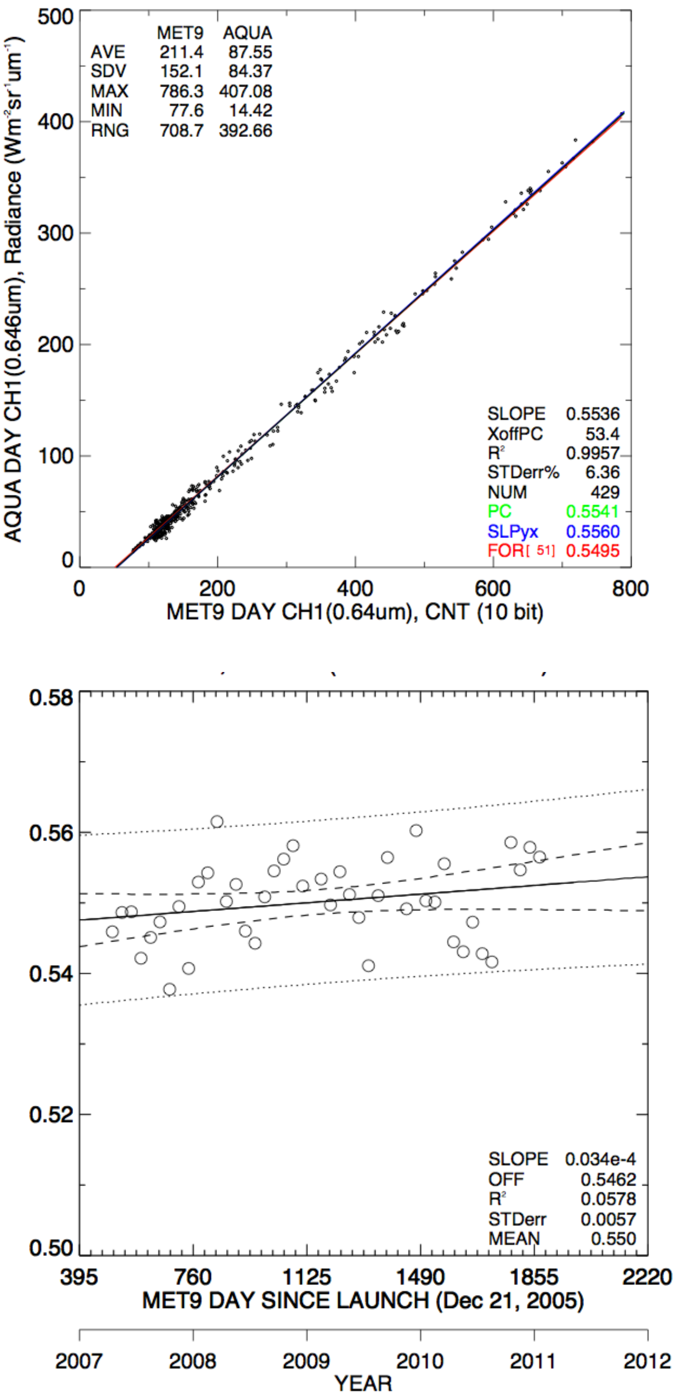

Figure 1: Upper panel: November 2007 monthly regression of Meteosat-9 counts and Aqua-MODIS gridded radiances. Lower panel: The Meteosat-9 monthly gains between 2007 and 2011.

The SEVIRI Solar Channel Calibration System

The Spinning Enhanced Visible and Infrared Imager (SEVIRI), onboard the Meteosat Second Generation geostationary satellites, observes the Earth in twelve spectral channels. Three spectral bands are centered on 0.6, 0.8 and 1.6 μm, whereas a fourth solar band is a broadband channel similar to the solar channel available on Meteosat First Generation. The observations are made within a 15 min repeat-cycle for a full-disk acquisition, and a 5 min repeat-cycle in rapid scan mode.

As for Meteosat First Generation, the MSG/SEVIRI radiometer does not have an on-board calibration system for the solar bands, so the operational calibration of these four channels relies exclusively on vicarious calibration. The current requirements on the solar band calibration are 10% accuracy in radiance for near real time applications, and 2% accuracy over a year for long term applications. In order to reach these objectives, the SEVIRI Solar Channel Calibration System (SSCC) has been developed at EUMETSAT (Goverts and Clerici 2004a, 2004b, and 2004c) and run since 2003. It uses as a calibration reference the simulated Top-Of-Atmosphere (TOA) radiances over a set of 18 bright and radiometrically stable desert sites, and 10 oceanic targets. These reference TOA radiances are compared with the observed TOA radiances. Desert sites are used for deriving the calibration coefficients, whereas oceanic targets are used for consistency checks.

This calibration reference is an estimate of the real TOA radiance computed with a radiative transfer model (a tailored version of the 6S model (Vermote et al. 1997), as available in 2003) and a set of state variables. In order to assess its accuracy, the calibration reference was evaluated against well-calibrated TOA measurements acquired by instruments such as ATSR-2, SeaWiFS, and VEGETATION. A detailed analysis done by Govaerts and Clerici (2004a) showed that the relative bias between observed and modeled TOA radiances does not exceed 3% with respect to ATSR-2 and SeaWiFS. This bias is about 5% with respect to VEGETATION. However, the calibration of VEGETATION relies on vicarious calibration, whereas ATSR-2 and SeaWiFS have on-board calibration devices. So, provided that a large number of observations are processed, the expected accuracy of the SEVIRI solar band calibration is ±5%.

Figure 1 provides an outline of the complete SSCC system. First, cloudy observations and non-admissible geometries are removed from the input data set. Once a target with admissible observations has been identified, the digital counts are extracted from the image. In order to minimize uncertainties in geo-locations, and to take into account all detectors of a specific band, the extraction is done for a box of pixels surrounding the target. A mean count value is calculated, together with a corresponding radiometric error and the range of counts over the extracted box. In a further stage, the reference radiative transfer model (based on the 6S model [Vermote et al. 1997]) is run for all illumination and viewing angles corresponding to the extracted observations. The calculated Top-Of-Atmosphere (TOA) radiances and their associated errors are accumulated over time for each target box. The corresponding calibration coefficients are derived using the reference TOA radiances and the associated observed counts.

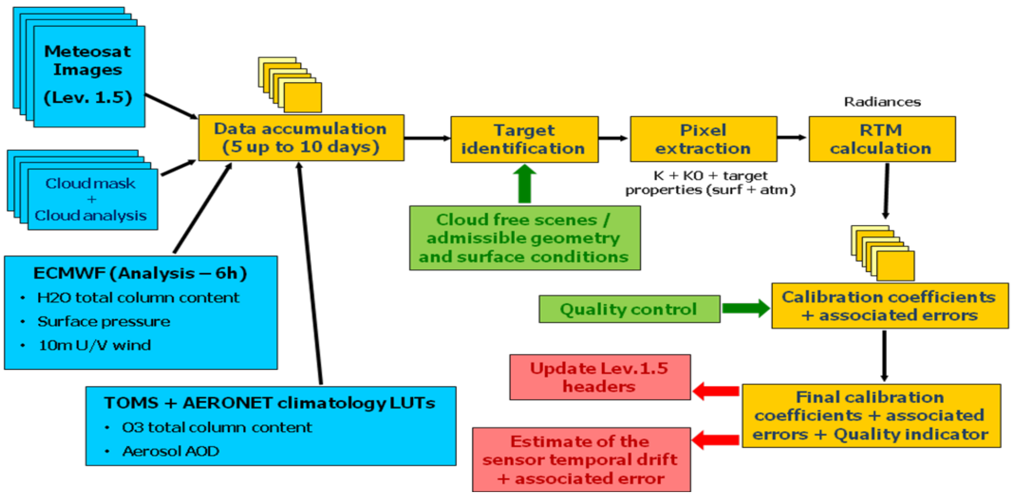

Figure 1: Diagram representing the SSCC system, as implemented at EUMETSA

A first screening of the retrieved calibration coefficients is performed to remove the outliers. Further, in order to reduce the impact of random errors, the weighted average over time of the remaining calibration coefficients is calculated, using the individual associated errors as weights. At this stage, a new screening of the data is performed to remove the results for the pixels where the estimated error is not acceptable and the remaining desert target data are used to estimate the offset value.

In a penultimate step, the temporally averaged data are spatially averaged over each target box. As the spectral properties of the processed desert pixels within a target box must be homogeneous, inconsistent pixels are removed after comparison with the mean value.

Finally, calibration coefficients are derived over ocean targets in order to check the consistency of the results obtained for desert targets. The coefficients retrieved from the sea targets should be in agreement within the uncertainty interval with the results from the desert targets unless the instrument response is nonlinear, or the sensor spectral response is not well characterized, or the modeled TOA radiances are not accurate enough. In order to assess any possible bias, a last consistency check is done by estimating for both desert and sea targets the offset value that defines the space count.

The long term drift of the instrument is assessed after assuming a linear degradation of the instrument gain. As a result, the value of this drift is derived by a linear regression of the final retrieved calibration coefficients since the launch of the satellite.

This vicarious calibration approach can be equally applied to the MVIRI instrument onboard the Meteosat First Generation platforms. SSCC is also expected to become the vicarious calibration algorithm for the solar channels of the future Meteosat Third Generation Flexible Combined Imager mission. However, more stringent requirements on the absolute calibration accuracy call for further improvements of the current system. Some of the needed improvement could be achieved by the definition of a more accurate reference, that is, a better modeling of the surface and atmospheric radiative processes. However, the current system could also benefit from the use of other targets such as the Moon and deep convective clouds. The developments of these latter methods are currently on going at Eumetsat. As the calibration reference is improved, there will be a clear possibility for reprocessing the Meteosat archive for the solar channels and improve the current calibration for all missions, all traceable to the same reference.

(by Dr. Sebastien Wagner, [EUMETSAT])

REFERENCES

Govaerts, Y. M. and M. Clerici, 2004a: Evaluation of radiative transfer simulations over bright desert calibration sites. *IEEE Trans. Geo. Remote Sens.*, **42(1)**, 176-187.

Govaerts, Y. M., M. Clerici, et al., 2004b: Operational Calibration of the Meteosat Radiometer VIS Band. *IEEE Trans. Geo. Remote Sens.*, **42(9),** 1900-1914.

Govaerts, Y. M., and M. Clerici, 2004c: *MSG-1/SEVIRI Solar Channels Calibration Commissioning Activity Report (EUMETSAT).*

Vermote, E.F., D. Tanré, J. L. Deuzé, M. Herman, and J. J. Morcrette, 1997: Second Simulation of the Satellite Signal in the Solar Spectrum, 6S: An Overview, *IEEE Trans. Geo. Rem. Sens.*, **35**, 675-686.

Vicarious Calibration for COMS Solar Band Using Cloud Targets

Two types of cloud modeling methods have been developed for the vicarious calibration of Korean geostationary satellite, Communication, Ocean and Meteorological Satellite (COMS), solar band. The first cloud modeling method uses cloud optical properties estimated from well-calibrated solar channel measurements for the TOA reflectance calculation. Moderate Resolution Imaging Spectroradiometer (MODIS) cloud products are used in this study, and thus MODIS solar channel sensors serve as a reference sensor. In the second cloud modeling method, deep convective cloud (DCC) targets are selected using the infrared (IR) brightness temperature threshold and homogeneity checks. Typical properties of DCC targets based on MODIS observations are then used for the radiative transfer simulations. More detailed description of those methods can be found in Sohn et al. (2009) and Ham and Sohn (2010).

Cloud modeling method with MODIS cloud products

For selecting cloud targets and performing radiative transfer simulation of them, collocated MODIS cloud products are used. In doing so, COMS and MODIS satellite measurements are averaged in a 0.5°×0.5° grid format and observation time differences up to 5 min between two sensors are considered. Applying MODIS cloud mask information, only the 0.5°-grid boxes that are filled entirely with cloud pixels are considered. In addition, grid boxes showing a cloud optical thickness (COT) greater than 5 are selected. For the selected cloud grid targets, sensor-reaching reflectances are simulated using collocated MODIS cloud products, such as COT, cloud effective radius, and cloud top pressure. In addition, grid-averaged cloud top temperature is used to determine the dominant cloud phase at a 0.5°-grid box. Then TOA reflectances are simulated under cloudy conditions by using the Santa Barbara Disort Radiative Transfer (SBDART; Ricchiazzi et al., 1998) model, implemented with 20 streams. Moreover, in the calculation of 0.5°-grid reflectances, the independent column approximation (LN-ICA) method (Oreopoulos and Davies, 1998) is adopted to remove 1-D simulation biases caused by subgrid variation of COT. Finally, simulated reflectances for the cloud targets are compared with COMS level 1B reflectance for the calibration monitoring.

Deep convective cloud (DCC) method

DCCs overshooting the tropical tropopause layer (TTL) are identified when the window channel (11 µm) brightness temperature (TB_{11}) ≤ 190 K. In addition, homogeneity checks are applied to avoid cloud edges or small-scale plumes, using standard deviations (STDs) of the visible reflectance and TB_{11} for the surrounding pixels over a 10 km × 10 km area. After selecting DCC targets, DCC properties are assumed in the radiative transfer model (RTM) based on the examination of DCC targets using Moderate Resolution Imaging Spectroradiometer (MODIS) cloud products (Sohn et al., 2009); i.e., COT is assumed 200, and effective radius is assumed 20 µm. Moreover, the cloud top and cloud base heights are assumed to be 15 km and 1 km, respectively. After describing cloud optical properties, COMS reflectance is simulated using the SBDART model, implemented with 20 streams. In the simulation, ice cloud phase is assumed since the uppermost parts of clouds overshooting the TTL mostly contains nonspherical ice particles. Finally, daily averaging of the target reflectances is performed to minimize simulation errors caused by instantaneous variations of cloud properties.

Figure 1 (below) represents COMS calibration results using two cloud modeling methods. Blue lines represent regression lines obtained from cloud modeling method with MODIS cloud products, while each cross represents daily averaged value for the DCC targets. Inter-satellite calibration results using MODIS 0.6-µm channel as a reference are also given as red lines. All three methods suggest a similar degree of biases around 9–10% in COMS Level 1B visible reflectances.

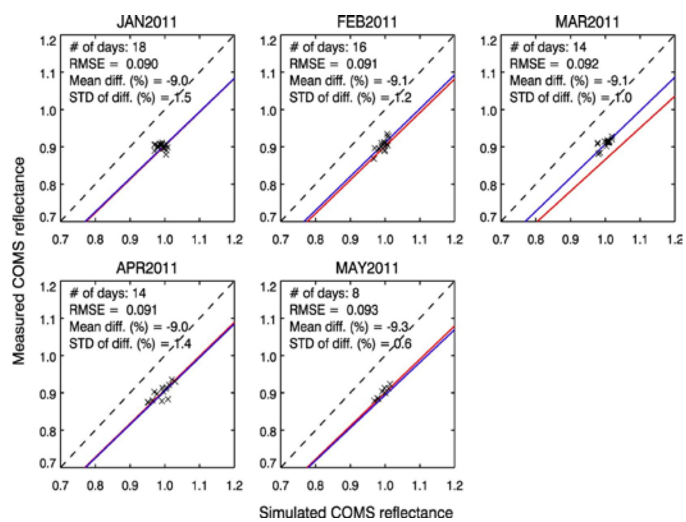

Figure 1. Regression lines from cloud modeling method with MODIS cloud products are represented as blue lines, while DCC calibration results are given with crosses. Regression lines obtained from inter-satellite calibration are also represented as red lines. Dashed lines are perfect matches.

(by Drs. Seung-Hee Ham and B.J. Sohn, [Seoul National University of South Korea])

REFERENCES

Ham, S.-H., and B. J. Sohn, 2010: Assessment of the calibration performance of satellite visible channels using cloud targets: application to Meteosat-8/9 and MTSAT-1R. *Atmos. Chem. Phys.*, **10(22)**, 11131-11149, doi: 10.5194/acp-10-11131-2010.

Oreopoulos, L. and R. Davies, 1998: Plane parallel albedo biases from satellite observations. Part II: Parameterizations for bias removal, J. Climate, **11**, 933–944.

Ricchiazzi, P., S. Yang, C. Gautier, and D. Sowle, 1998: SBDART: A research and teaching software tool for plane-parallel radiative transfer in the Earth's atmosphere. *Bull. Amer. Meteor. Soc.*, **79**, 2101–2114.

Sohn, B.-J., S.-H. Ham, and P. Yang, 2009: Possibility of the visible-channel calibration using deep convective clouds overshooting the TTL. *J. Appl. Meteor. Climatol.*, **48,** 2271-2283.

Star-Based Calibration Techniques – Application to GSICS Inter-Calibration of Solar Channels of Satellite Radiometers: Part I

Techniques that are currently in use to monitor the degradation rate of the responsivity in the visible (solar) channel of the Imager carried by NOAA's Geostationary Operational Environmental Satellite (GOES) can be employed to support the inter-calibration efforts of the GSICS. In this two-part report, we will describe star-based calibration techniques developed at NOAA/NESDIS over the past decade. The basic assumption underlying the techniques is that a change in the measured brightness of a star whose brightness is known to be constant must be the result of a change in the instrument's responsivity.

In Part 1, we present our principal method of detecting the presence of a star in the Imager's field of view and determining the strength of its signal in units of digital instrument output. We then show a time series of such star signals and discuss briefly the concept of estimating the rate of degradation of the instrument's responsivity from the trajectory of the time series. In Part 2, we shall describe more fully how the time series of a collection of stars can be used to estimate the degradation rate of the responsivity on the absolute radiance scale by linking the star data to the Moderate-resolution Imaging Spectroradiometer (MODIS) observations. In doing so, we will move beyond the mission of monitoring instrument responsivity toward the areas of inter-satellite comparison and absolute calibration.

The visible channel of the Imager on a GOES satellite observes stars at regular time intervals as a part of the operational process for determining the Imager's orbit and attitude. Figure 1 illustrates the crossing of a star image over the detectors of a visible channel in a star sensing operation. The visible channel is equipped with a linear array of eight detectors oriented essentially in the north-south direction. In Figure 2, the two plots (termed "profiles") show the intensity of the star light measured by Detector 5 and Detector 6 as each detector registered the crossing of a portion of the star image that illuminated both detectors. Measurements are received from each of the eight detectors at the rate of 21,800 pixels per second. To compact the volume of such data to a manageable size, each block of 400 pixels is summed to produce a measured intensity of a *super-pixel*, which takes the place of the original 400 pixels. Each data point in Figure 2 is actually the intensity of a super-pixel. The units on the abscissa are Detector Time Units (DTU), where one DTU is 400/21800 second. The units on the ordinate are Detector Pixel Units (DPU), where one DPU is one (digital) count output of the original pixel on the measuring channel. For each star look, the eight detector profiles (expressed in super-pixels), together with the time tag of the star look and the identification number of the star, are the principal required input data in our calibration method.

We employ an algorithm modified from the GOES operational procedures to detect the presence of a star image on the profile of a detector (GOES OGE 2000). In this algorithm, each super-pixel profile is smoothed by using a 12-point moving-average process. A group of consecutive pixels in a smoothed profile is declared to be that of a star image if the values of the pixels are above a certain threshold level and the number of pixels in the group is larger than certain lower bound.

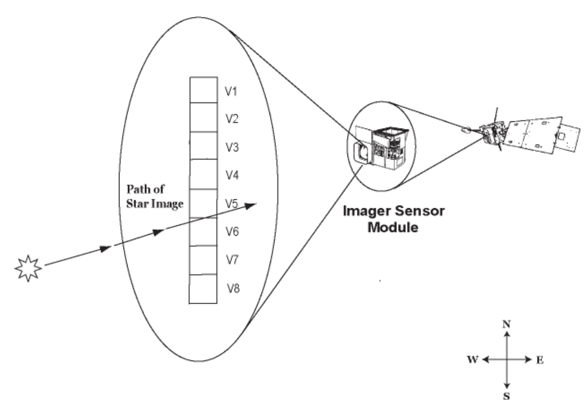

Figure 2. The eight detectors of the visible channel of a GOES Imager conducting a star look.

If star images have been detected on some of the detectors, we compute a star signal by first returning to the original detector profiles where each point is a super-pixel. Now we regard the linear array of eight detectors (Figure 1) as one integral detector where the image of the star moved across this single detector. We first combine the super-pixel profiles that contain star images into one composite signal profile by summing at each time mark the measurements from each such profile. The data in this composite profile are then made absolute relative to the zero signal of space by subtracting the baseline (space signal) from them. The baseline level is computed as the result of a median filter applied to this sequence of points. Finally, each point in the sequence is divided by 400 to transform the pixel amplitude from that of a super-pixel to that of an original pixel measured on a detector.

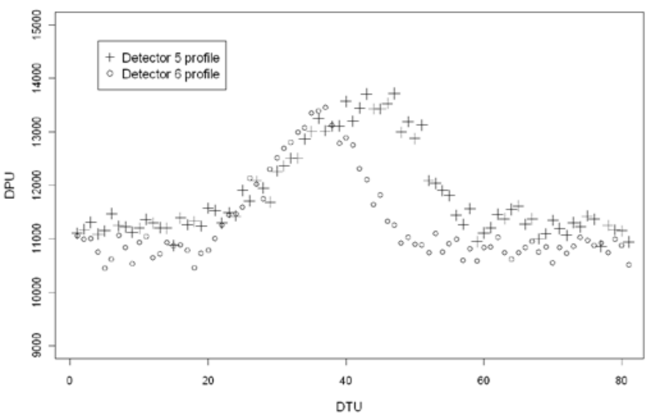

Figure 3. Measurements received from Detector 5 (+ symbols) and Detector 6 (circles) of the visible channel of the Imager of GOES-12, in a star look of β-Cnc, conducted on May 14, 2007. X-axis represents time, Y-axis the GOES measurement of the star light; see text for detailed explanation of coordinates.

Once a composite profile has been computed, a search to estimate the peak value is carried out. A sequence of moving averages across the profile is computed. The number of pixels included in the average is a predetermined parameter with the default value of 8. Calling the maximum value in this set of averages the peak value, we define this peak value to be the *signal of the star*. Throughout the process of detecting a star image and computing a star signal, we conduct certain checks to determine whether the process should be continued. At this time, there are eight conditions for rejecting a star look. One such condition is that more than one star image entered a detector.

Figure 3 shows the plot of a 14-month time series of star signals of the star β-Cnc (in dots), observed by the Imager on GOES-13. We have excluded star signals obtained within five hours on each side of the local midnight. Signals measured in this period are usually low in value, due to distortion of the scan mirror caused by increased heating by the sun (Bremer et al. 1998). For estimating an annual rate of change in the responsivity of the channel, one approach we use is to fit exponential functions ($y = \beta e^{-At}$) to the star-signal time series of a chosen group of stars, where time *t* is measured in days since after the launch date of the satellite or the date when the satellite started its regular operation. For the time series of Figure 3, the exponential fit gives an annual degradation rate *A*=5.06%. The average annual degradation rate computed from 45 chosen stars over approximately the same period yields a rate of $\hat{A}$=5.05%, with a standard error of the mean of 0.23%.

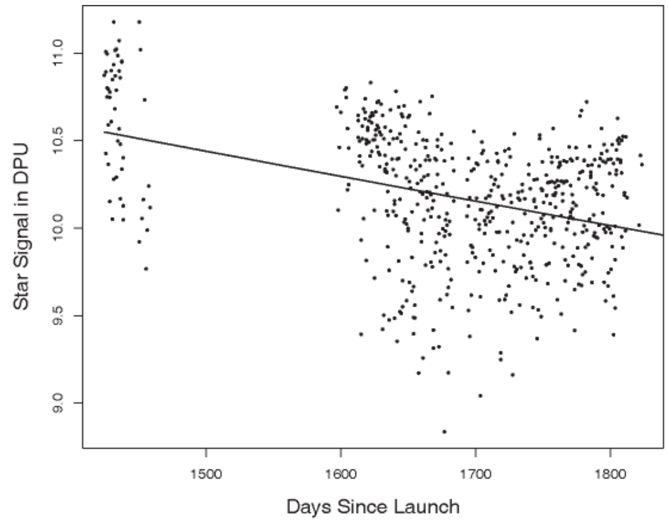

Figure 3. A time series of star signals of β-Cnc from GOES-13 and the exponential fit to the data. The data were obtained over the period April 16, 2010 (shortly after the satellite started regular operations), to May 20, 2011.

The method described in this report evolved from several earlier star calibration methods that have continued to serve as robust and stable visible-channel methods for monitoring degradation. In particular, the method, denoted as star calibration Method 2 (Chang et al. 2004), has been providing regular degradation estimates since the early 2000's. In this method, we depend on the operational GOES Orbit and Attitude Tracking System (OATS) to report the presence of star images and compute the star signals from the data of the star looks. After quality screening the star signals, we fit exponential functions to their time series to estimate the degradation rates. However, the OATS algorithms are not optimized for calculating the star signals, as they had been developed to determine pixel location of the star, not the star signal. Therefore, in the mid-2000's, we developed the current method to become independent of the OATS processing and improve the accuracy of the computed star signals. Method 2, however, continues to provide the degradation-rate reports that we disseminate to users.

The estimates of responsivity degradation rates for Imager visible channels of GOES satellites based on the star observations are available on http://www.star.nesdis.noaa.gov/smcd/spb/fwu/homepage/GOES_star_cal.php.

(by Drs. I. Chang, C. Dean, Z. Li, M. Weinreb, X. Wu and F. Yu, [NOAA])

REFERENCES

GOES IJK/LM, Operation Ground Equipment (OGE) Interface Specification, DRL 504-02, Part 1, June 2000.

Bremer, J.C., J.G. Baucom, H. Vu, M. P. Weinreb, and N. Pinkine, 1998: Estimation of long-term throughput degradation of GOES 8 & 9 visible channels by statistical analysis of star measurements", *Earth Observing Systems III*, *Proc. SPIE* **3439,** pp. 145-154.

Chang, I-L., D. Crosby, C. Dean, M. Weinreb, P. Baltimore, J.Baucom, and D. Han, 2004: Data selection criteria in star-based monitoring of GOES imager visible-channel responsivities, *Imaging Spectrometry X*, *Proc. SPIE* **5546,** pp. 253-261.

News in this Quarter

IEEE TGRS Special Issue on "Inter-Calibration of Satellite Instruments"

Call for Papers: This special issue of the Transactions on Geoscience and Remote Sensing (TGRS) will focus on how inter-calibration and comparison between sensors can provide an effective and convenient means of verifying post-launch sensor performance and correcting the differences. The guest editors invite submissions that explore calibration methods including, but not limited to, pseudo-invariant calibration sites, instrumented sites, simultaneous nadir observations and other ray-matching comparisons, lunar and stellar observations, deep convective clouds, liquid water clouds, Rayleigh scattering and Sun glint. The inter-calibration results should focus on rigorous quantification of bias and associated sources of uncertainty from different sensors, crucial for long-term studies of the Earth. The goal of this special journal issue is to capture the state-of-the-art methodologies and results from inter-calibration of satellite instruments, including full end-to-end uncertainty analysis. Accordingly, it will become a reference anthology for the remote sensing community.

Paper submission deadline: 21 February 2012

Guest Editors: Gyanesh Chander [SGT/USGS], Tim Hewison [EUMETSAT], Nigel Fox [NPL], Xiangqian "Fred" Wu [NOAA], Xiaoxiong "Jack" Xiong [NASA], William J. Blackwell [MIT/LL]

Just Around the Bend …

GSICS-Related Meetings

- 18th Conference on Satellite Meteorology, Oceanography and Climatology/First Joint AMS-Asia Satellite Meteorology conference, which will be held as part of the 92nd American Meteorological Society Annual Meeting, 22-26 January 2012 in New Orleans, LA, USA.

- The 7th GSICS Research Working Group (GRWG) and 6th GSICS Data Working Group (GDWG) meeting will be held at the National Satellite Meteorological Center (NSWC) of China Metrological Administration (CMA), Beijing from 5 to 9 March 2012.

GSICS Publications

Anderson, T., et al: 2011. Intercalibration and evaluation of ResourceSat-1 and Landsat-5 NDVI. *Can. J. of Remote Sens.*, online only.

Jeong, M-J., et al. 2011: Impacts of cross-platform vicarious calibration on the deep blue aerosol retrievals for Moderate Resolution Imaging Spectroradiometer aboard Terra, *IEEE Trans. Geo. Remote Sens.*, **49(12)**, 4877-4888.

Yang, H., et al. 2011: The FengYun-3 microwave radiation Imager on-orbit verification, *IEEE Trans. Geo. Remote Sens.*, **49(11),** 4552-4560.

Please send bibliographic references of your recent GSICS-related publications to Fangfang.Yu@noaa.gov.

With Help from our Friends:

The *GSICS Quarterly* Editor would like to thank those individuals who contributed articles and information to this newsletter. The Editor would also like to thank Dr. George Ohring for the careful proofreading of the articles, our European Correspondent, Dr. Tim Hewison of EUMETSAT, and Asian Correspondent, Dr. Yuan Li of CMA, in helping to secure and edit articles for publication.

Submitting Articles to GSICS Quarterly: The *GSICS Quarterly* Press Crew is looking for short articles (<1 page), especially related to cal/val capabilities and how they have been used to positively impact weather and climate products. Unsolicited articles are accepted anytime, and will be published in the next available newsletter issue after approval/editing. **Please send articles to Fangfang.Yu@noaa.gov.**